Available online at www.sciencedirect.com

ScienceDirect

journal homepage: www.jfda-online.com

Original Article

Application of novel Ni(II) complex and ZrO_2 nanoparticle as mediators for electrocatalytic determination of N-acetylcysteine in drug samples

Hassan Karimi-Maleh [a,*], *Mehdi Salehi* [b], *Fatemeh Faghani* [b]

[a] *Department of Chemical Engineering, Laboratory of Nanotechnology, Quchan University of Advanced Technology, Quchan, Iran*

[b] *Department of Chemistry, College of Science, Semnan University, Semnan, Iran*

ARTICLE INFO

Article history:
Received 19 September 2016
Received in revised form
27 December 2016
Accepted 18 January 2017
Available online 13 February 2017

Keywords:
electrocatalysis
modified electrode
N-acetylcysteine
Ni(II) complex
ZrO_2 nanoparticle

ABSTRACT

The electrooxidation of N-acetylcysteine (N-AC) was studied by a novel Ni(II) complex modified ZrO_2 nanoparticle carbon paste electrode [Ni(II)/ZrO_2/NPs/CPE] using voltammetric methods. The results showed that Ni(II)/ZrO_2/NPs/CPE had high electrocatalytic activity for the electrooxidation of N-AC in aqueous buffer solution (pH = 7.0). The electrocatalytic oxidation peak currents increase linearly with N-AC concentrations over the concentration ranges of 0.05–600μM using square wave voltammetric methods. The detection limit for N-AC was equal to 0.009μM. The catalytic reaction rate constant, k_h, was calculated (7.01×10^2 M^{-1} s^{-1}) using the chronoamperometry method. Finally, Ni(II)/ZrO_2/NPs/CPE was also examined as an ultrasensitive electrochemical sensor for the determination of N-AC in real samples such as tablet and urine.

1. Introduction

N-Acetylcysteine (N-AC) comes from the amino acid L-cysteine, which has many uses as medicine. N-AC is suggested to counteract paracetamol and CO poisoning and is also used for chest pain, bile duct blockage in infants, amyotrophic lateral sclerosis, Alzheimer's disease, allergic reactions to the antiseizure drug phenytoin, and eye infection (keratoconjunctivitis). N-AC is a building block for antioxidants [1]. N-AC overdose can be harmful because of its side effects such as diarrhea, upset stomach, skin rash, and fatigue [2]. A variety of analytical methods have been suggested for determination of N-AC in real samples such as spectrophotometry [3–6], chromatography [7–9], flow injection [10], fluorimetry [11], and electrochemical methods [12,13]. Compared to other analytical methods, electrochemical techniques are proposed for pharmaceutical, biological, and environmental detection owing to their fast response, low cost, good selectivity, and high sensitivity [14–25].

Room temperature ionic liquids are salt liquids at room temperature with special properties such as high conductivity, nonvolatility, large electrochemical potential window,

* *Corresponding author*. Department of Chemical Engineering, Laboratory of Nanotechnology, Quchan University of Advanced Technology, Quchan, Iran.
E-mail address: h.karimi.maleh@gmail.com (H. Karimi-Maleh).

http://dx.doi.org/10.1016/j.jfda.2017.01.003

chemical stability, low vapor pressure, and good thermal stability [26–30]. Room temperature ionic liquids are good binders and a suitable mediator for modification of electrochemical sensor in voltammetric and amperometric analysis [31–36].

Nano-based materials represent a new era for the development of novel modified sensors because of their unique properties such as good electrical conductivity [37–40]. Nano-based materials, especially metal-based nanoparticles (NPs), have been successfully used as modifiers to obtain very low detection limits in electrochemical sensors [41–43].

In the present work, we investigated the synthesis and application of a new Ni(II) complex, [NiII(L)(MeIm)], where H_2L is (*E*)-2-(5-bromo-2-hydroxybenzylideneamino)phenol and MeIm is *N*-methyl imidazole, as a novel mediator for the electrocatalytic determination of *N*-AC using voltammetric methods. Ni(II)/ZrO_2/NPs/CPE is ultrasensitive in the detection of *N*-AC in real samples. To the best of our knowledge, this study is the first to report on the application of [NiII(L)(MeIm)] as an electrocatalyst in the voltammetric determination of biological or pharmaceutical samples.

2. Experimental

2.1. Chemicals and instrumentation

N-AC, zirconium(IV) chloride, and phosphoric acid were purchased from Sigma-Aldrich. Graphite powders, sodium hydroxide, and paraffin oil, were purchased from Merck (Germany). Phosphate-buffered saline solutions (0.1M) with different pH values were used for the pH optimization study.

X-ray powder diffraction studies were carried out using an STOE diffractometer with Cu–Ka radiation (l = 1.54 Å). Voltammetric investigation was performed in an electroanalytical system, Autolab PGSTAT 12, potentiostat/galvanostat connected to a three-electrode cell, Metrohm Model 663 VA stand linked with a computer (Pentium IV), and with Autolab software. The system was run on a PC using GPES and FRA 4.9 software.

2.2. Synthesis of [Ni^{II}(L)(MeIm)]

In a typical experiment, a solution of 0.146 g (0.5 mmol) of (*E*)-2-(5-bromo-2-hydroxybenzylideneamino)phenol (H_2L) in 10 mL methanol was placed in a round bottom two-necked flask equipped with a magnetic stirrer, a dropping funnel, and a reflux condenser. This solution was heated, and then a solution of $Ni(OAc)_2{\cdot}4H_2O$ (0.5 mmol) in 10 mL methanol was added dropwise from the dropping funnel. The reaction mixture immediately turned bright red. Then, a few drops of *N*-methyl imidazole (MeIm) was slowly added to the solution. The reaction mixture was stirred and heated at a gentle reflux for a further 3 hours. The single crystals suitable for X-ray data collection were obtained by slow evaporation of the methanol solution after 4 days. The crystals were filtered off, washed with a small amount of cold methanol, and dried under vacuum. Yield: 70%. Red color crystals. Mol. wt.: 430.90 Anal. Calcd. for $C_{17}H_{14}BrN_3NiO_2$: C, 47.38; H, 3.27; N, 9.75. Found: C, 47.22; H, 3.18; N, 9.70%. Fourier transform-infrared: ν_{max} (cm^{-1}) (KBr): 1596 (C=N), 1095 (ClO_4). UV–Vis: λ_{max} (nm) (ε, M^{-1} cm^{-1}) (CH_3CN): 261 (70,000), 325 (25,000), 444 (35,000). ^1H nuclear magnetic resonance: 8.03(s, 1H), 7.65 (s, 1H), 7.54 (dd, 1H), 7.48 (d, 1H), 7.23 (dd, 1H), 7.07 (d, 1H), 7.04 (t, 1H), 6.84 (t, 1H), 6.82 (s, 1H), 6.75 (dd, 1H), 6.55 (d, 1H). The synthetic procedure for the preparation of the complex is shown in Figure 1.

2.3. Synthesis of ZrO_2/NPs

To synthesize the ZrO_2/NPs, in a typical experiment, a 0.5M aqueous solution of zirconium (IV) chloride and a 2.5M aqueous solution of sodium hydroxide were prepared in distilled water. Under continuous stirring, the beaker containing sodium hydroxide solution was heated at a temperature of about 35°C. The zirconium (IV) chloride solution was added dropwise to the heated solution under high-speed stirring. The precipitated Zr hydroxide was cleaned with deionized water and ethanol, then calcined at 800°C for 1.5 hours.

2.4. Preparation of real samples

Ten *N*-AC tablets were grinded. Then, the tablet solution was prepared by dissolving a suitable amount of the powder in 100 mL water by ultrasonication. Then, 0.1 mL of the solution was diluted with the buffer solution (pH 7.0) in a 10-mL volumetric flask. The *N*-AC content was analyzed by the proposed method using the standard addition method. The human urine samples were analyzed after 2 hours of their sampling, except when stated otherwise. The prepared samples were taken from humans and were used for measurements after they were centrifuged (2500 rpm, room temperature) and diluted four times with phosphate-buffered saline without any further pretreatment. Pharmaceutical and water sample were prepared without any revision.

2.5. Preparation of voltammetric sensor

A 5.0% (w/w) Ni(II) complex spiked graphite and ZrO_2/NPs powders was made by dissolving the given quantity of Ni(II) complex in diethyl ether and hand mixing with 90.0% (w/w) of graphite powder and 5.0% (w/w) ZrO_2/NPs with a mortar and pestle. The solvent was evaporated by stirring, and mixture of ZrO_2/NPs, ZrO_2/NPs spiked carbon powder plus paraffin oil was blended by hand mixing. The resulting paste was inserted in the bottom of a glass tube. The electrical connection was implemented by a copper wire lead fitted into a glass tube.

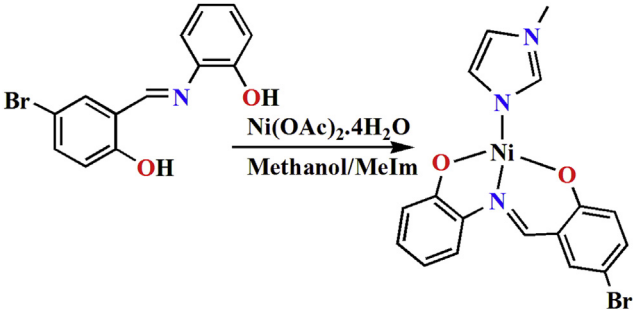

Figure 1 – Synthetic procedure for the preparation of complex.

3. Results and discussion

3.1. ZrO_2 nanopowder and electrode surface characterization

The X-ray powder diffraction (XRD) patterns of the ZrO_2/NPs are shown in Figure 2A. X-ray diffraction studies confirmed that the synthesized materials were ZrO_2 in tetragonal form [44]. The synthesized ZrO_2/NPs diameter was calculated using the Debye–Scherrer equation:

$$D = K\lambda/(\beta \cos\theta), \quad (1)$$

where λ is the wavelength (λ = 1.542 Å) (CuKα), β is the full width at half-maximum of the line, and θ is the diffraction angle. The average particle size of the sample was found to be 20 nm. The morphology of the as-grown nanostructures was characterized by scanning electron microscopy (SEM) methods. A typical SEM image of the ZrO_2 nanopowder is shown in Figure 2B. The results confirmed the synthesis of ZrO_2 nanopowder.

The SEM images of carbon paste electrode and Ni(II)/ZrO_2/NPs/CPE are shown in Figures 2C and 2D, respectively. As can be seen, Ni(II) and ZrO_2/NPs disperse at a surface of graphite layers.

3.2. Voltammetric investigation

The electrochemical behavior of [Ni^{II}(L)(MeIm)] was studied using cyclic voltammetry at the surface of Ni(II)/ZrO_2/NPs/CPE (Figure 3). The obtained data showed reproducible, well-defined, anodic and cathodic peaks with E_{pa}, E_{pc}, and E^0

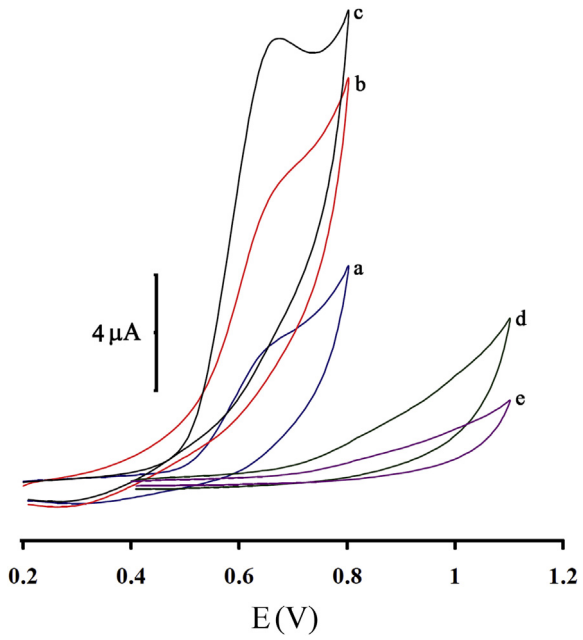

Figure 3 – Cyclic voltammograms of (a) 0.1M PBS at Ni(II)/ZrO_2/NPs/CPE; (b) 0.1M PBS plus 400.0μM N-AC at Ni(II)/CPE; (c) 0.1M PBS plus 400.0μM N-AC at Ni(II)/ZrO_2/NPs/CPE, and (d) 0.1M PBS plus 400.0μM N-AC at ZrO_2/NPs/CPE. Conditions: scan rate of 20 mV s^{-1} and pH 7.0. CPE = carbon paste electrode; N-AC = N-acetylcysteine; NP = nanoparticle; PBS = phosphate-buffered saline.

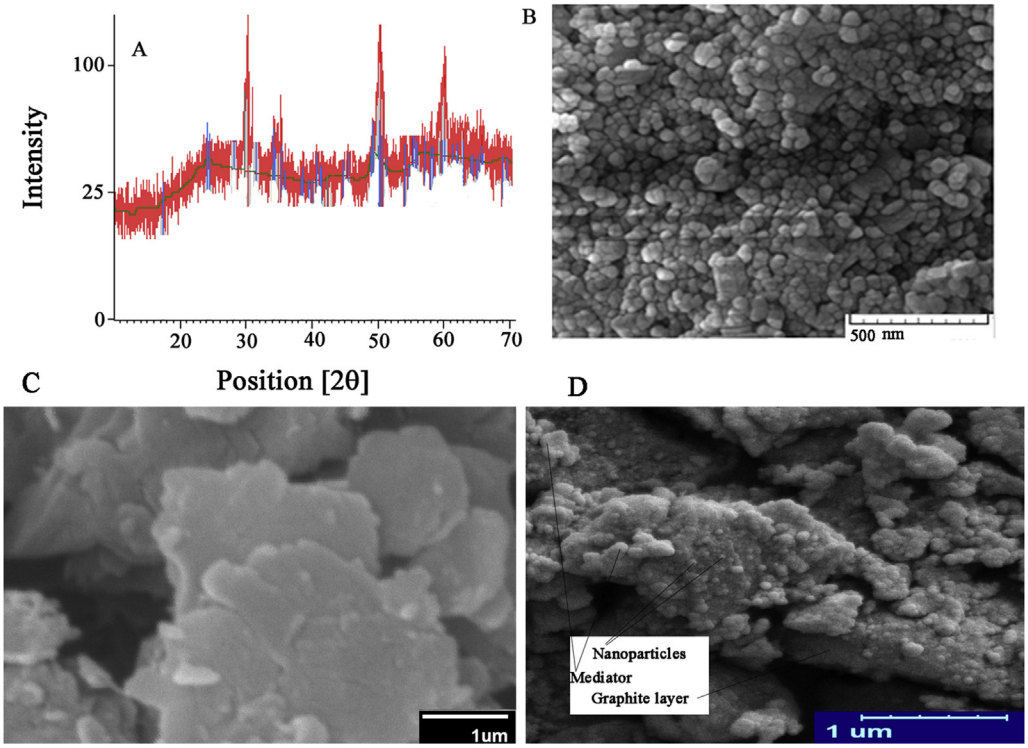

Figure 2 – (A) XRD patterns of as-synthesized ZrO_2/NPs. (B) SEM image of as-synthesized ZrO_2/NPs. (C) SEM image of carbon paste electrode. (D) SEM image of Ni(II)/ZrO_2/NPs/CPE. CPE = carbon paste electrode; NP = nanoparticle; SEM = scanning electron microscopy; XRD = X-ray diffraction.

values of 0.64, 0.35, and 0.495 V versus Ag/AgCl/KCl_{sat}, respectively. The observed peak separation potential, $\Delta E_p = (E_{pa} - E_{pc})$ of 290 mV, was greater than the value of 59/n mV expected for a reversible system, suggesting that the redox couple of Ni(II)/Ni(III) in the Ni(II)/ZrO_2/NPs/CPE has a quasi-reversible behavior in an aqueous medium.

The effect of the potential scan rate (υ) on electrochemical properties of the Ni(II)/ZrO_2/NPs/CPE was also studied by cyclic voltammetry (Figure S1, insert; Supplementary information data). Plots of the anodic peak currents (I_p) was linearly dependent on the scan rate at the range of 5–500 mV/s (Figure S1), indicating that the redox process of Ni(II) complex at the Ni(II)/ZrO_2/NPs/CPE has a diffusionless nature.

Figure 3 depicts the cyclic voltammetric responses from the electrocatalytic oxidation of 400μM *N*-AC at Ni(II)/ZrO_2/NPs/CPE (curve c), at Ni(II)/CPE (curve b), at ZrO_2/NPs/CPE (curve d), and at CPE (curve e). As can be seen, the oxidation peak potential for *N*-AC at Ni(II)/ZrO_2/NPs/CPE (curve c) and at Ni(II)/CPE (curve b) was about 650 mV, whereas it was about 850 mV at ZrO_2/NPs/CPE (curve d). At the unmodified CPE, the peak potential of *N*-AC was about 880 mV (curve e). From these results, it was concluded that the best electrocatalytic effect (Figure 4) for *N*-AC oxidation was the one observed at Ni(II)/ZrO_2/NPs/CPE (curve c).

Figure S2 (Supplementary information data) shows the effect of scan rate on electrocatalytic oxidation of *N*-AC at a surface of Ni(II)/ZrO_2/NPs/CPE. As can be seen, good linear relationship between the peak current (I_{pa}) and square root of scan rate ($\upsilon^{1/2}$) were calculated, which indicated a diffusion-controlled electrochemical process.

The Tafel plot was used to obtain information about the rate-determining step (Figure S3; Supplementary information data) in oxidation of *N*-AC at a surface of Ni(II)/ZrO_2/NPs/CPE. The slope of the Tafel plot was equal to $2.3RT/n(1-\alpha)F$, which reached 0.1814 V/decade and 0.1523 V/decade for scan rates 6.0 mV s^{-1} and 14 mV s^{-1}, respectively. So, we obtained the mean value of 0.64.

Double potential step chronoamperometry was used for the determination of the diffusion coefficient GSH. Figure S4A (Supplementary information data) shows the current–time curves of Ni(II)/ZrO_2/NPs/CPE by setting the electrode potential at 200 mV (first step) and 800 mV (second step) for 300μM and 500μM of *N*-AC. As can be seen, there is not any net anodic current corresponding to the oxidation of the Ni(II) complex in the presence of *N*-AC. Also, the forward and backward potential step chronoamperometry for the Ni(II) complex in the absence of *N*-AC shows a symmetrical chronoamperogram with an equal charge consumed for the reduction and oxidation of the Ni(II) complex at the surface of CPE (Figure S4D, a; Supplementary information data). By contrast, in the presence of *N*-AC, the charge value associated with forward chronoamperometry is significantly greater than that observed for backward chronoamperometry (Figure S4D,

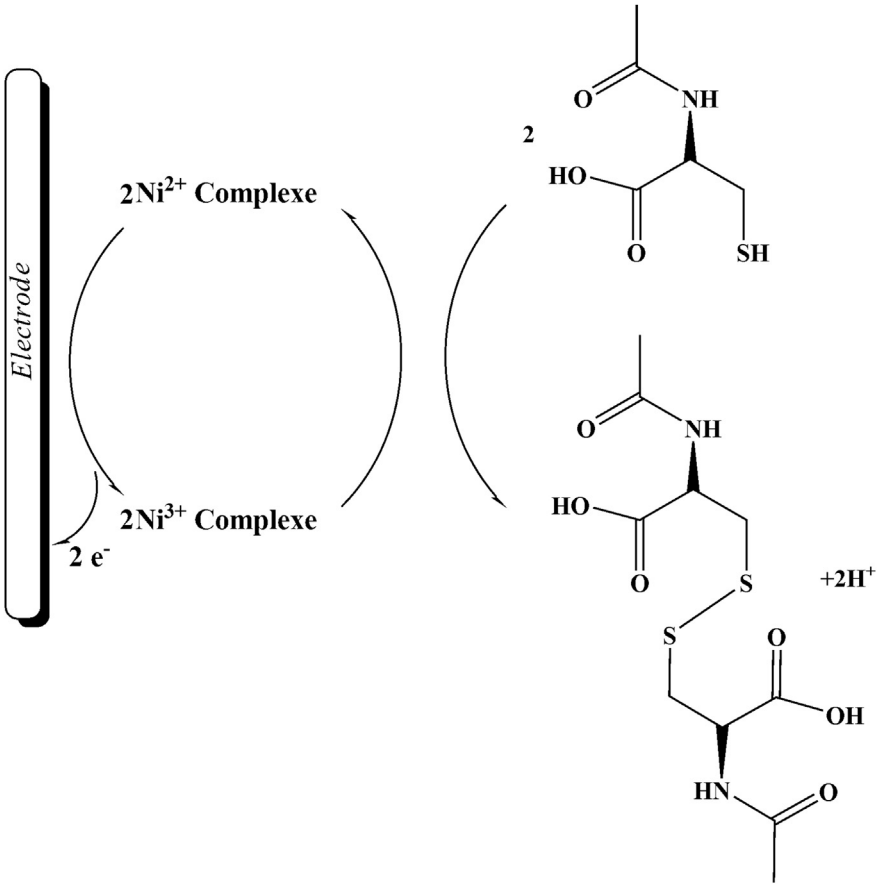

Figure 4 – Proposed response mechanism of the sensor based on Ni(II)/ZrO_2/NPs, for the catalytic electrooxidation of *N*-AC. *N*-AC = *N*-acetylcysteine; NP = nanoparticle.

b′–c′; Supplementary information data). The slope of the linear region of Cottrell's plot can be used to estimate the diffusion coefficient of *N*-AC (Figure S4B; Supplementary information data). The mean value of *D* for *N*-AC was found to be 2.97×10^{-5} cm^2 s^{-1}.

The rate constant for the chemical reaction between *N*-AC and redox sites in Ni(II)/ZrO_2/NPs/CPE, k_h, can be evaluated by chronoamperometry according to the method described by Galus [45]. From the values of the slopes an, average value of k_h was found to be $k_h = 7.01 \times 10^2$ M^{-1} s^{-1} (Figure S4C; Supplementary information data). The value of k_h explains as well as the sharp feature of the catalytic peak observed for catalytic oxidation of *N*-AC at the surface of Ni(II)/ZrO_2/NPs/CPE.

3.3. Dynamic range and limit of detection

Square wave voltammetry was used to determine *N*-AC (Figure 5, insert). The plot of the peak current versus *N*-AC concentration was linear for 0.05–600μM of *N*-AC (Figure 5).

The lower detection limit, C_m, was obtained by using the equation $C_m = 3s_b/m$, where s_b is the standard deviation of the blank response (μA) and *m* is the slope of the calibration plot. The data analysis presents the value of lower limit detection of *N*-AC to be 0.009μM.

3.4. Interference studies

The influence of various substances as potential interference compounds on the determination of *N*-AC under the optimum conditions with 20.0μM *N*-AC at pH 7.0 was studied. The tolerance limit was defined as the maximum concentration of the interfering substance that caused an error of less than 5% for the determination of *N*-AC. The results are given in Table 1 and show that the peak current of *N*-AC is not significantly affected by all conventional cations, anions, and organic substances.

3.5. Real sample analysis

The practical application of Ni(II)/ZrO_2/NPs/CPE was tested by measuring the concentrations of *N*-AC in tablet and urine samples. The standard addition technique was used for the determination of *N*-AC, and obtained data were compared with other published sensors [46]. The results obtained for the real samples are summarized in Table 2. These experiments demonstrated the ability of Ni(II)/ZrO_2/NPs/CPE for determination of *N*-AC with high electrocatalytic effect and good reproducibility.

3.6. Stability and reproducibility

The reproducibility and stability of Ni(II)/ZrO_2/NPs/CPE was studied by measurements of 10.0μM *N*-AC. We detected 1.5% relative standard deviation (RSD%) for seven successive analysis. Meanwhile, the repeatability of the Ni(II)/ZrO_2/NPs/CPE was checked using seven different electrodes. The results

Table 1 – Interference study for the determination of 20.0μM *N*-acetylcysteine (*N*-AC).

Species	Tolerance limits ($W_{Substance}/W_{N\text{-}AC}$)
Glucose, sucrose, glycine, methionine, alanine, Glutamic acid and Isolucin	1000
Ascorbic acid,[a] NO_3^-, SO_4^{2-}, Zn^{2+}, Li^+	500
Starch	Saturation

[a] Ascorbic acid interference can be minimize using ascorbic oxidase.

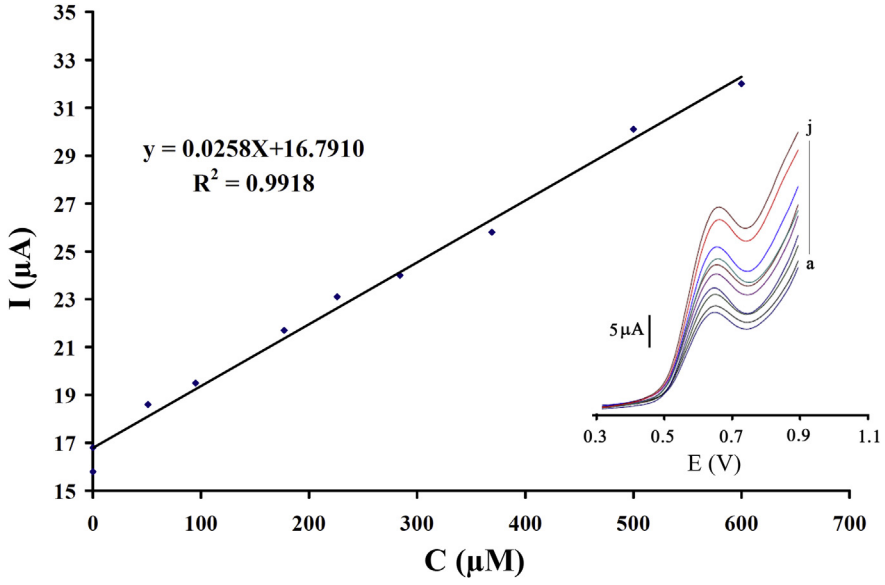

Figure 5 – The plots of the electrocatalytic peak current as a function of *N*-AC concentration. Inset shows the SWVs of Ni(II)/ZrO_2/NPs/CPE in 0.1M PBS (pH 7.0) containing different concentrations of *N*-AC. From inner to outer correspond to 0μM, 0.05μM, 50μM, 95μM, 177μM, 225μM, 2850μM, 370μM, 500μM, and 600μM of *N*-AC. CPE = carbon paste electrode; *N*-AC = *N*-acetylcysteine; NP = nanoparticle; PBS = phosphate-buffered saline; SWV = square wave voltammetry.

Table 2 – Determination of N-acetylcysteine (N-AC) in real samples at pH 7.0 ($n = 3$).

Sample	Added (μM)	Expected (μM)	N-AC found (μM)	Published method (μM)	F_{ex}	F_{tab}	t_{ex}	$t_{tab\ (95\%)}$
Tablet	—	10.00	9.85 ± 0.63	10.35 ± 0.73	8.5	19.0	1.8	3.8
	5.00	15.00	15.45 ± 0.73	15.65 ± 0.86	10.5	19.0	2.8	3.8
Urine	—	—	<limit of detection	<limit of detection	—	—	—	—
	20.00	20.00	20.85 ± 0.93	21.05 ± 1.11	13.8	19.0	3.1	3.8
	30.00	30.00	29.55 ± 0.85	30.65 ± 0.95	11.5	19.0	2.9	3.8
Pharmaceutical serum	—	—	<limit of detection	<limit of detection	—	—	—	—
	10.00	10.00	10.45 ± 0.53	9.83 ± 0.71	8.1	19.0	1.2	3.8
Water sample	—	—	<limit of detection	<limit of detection	—	—	—	—
	50.00	50.00	50.87 ± 0.93	50.93 ± 1.03	12.1	19.0	3.4	3.8

showed an RSD% of 2.9%. Furthermore, the stability of Ni(II)/ZrO_2/NPs/CPE was examined by storing the electrode in the laboratory. Then, the Ni(II)/ZrO_2/NPs/CPE was used for the analysis of 10.0μM N-AC using square wave voltammetry. We detected 97% of its initial response after 20 days and 93% of its initial response after 45 days.

4. Conclusion

An ultrasensitive and novel electrochemical sensor was developed for the determination of N-AC. The novel mediator, [Ni^{II}(L)(MeIm)] complex, showed excellent electrocatalytic effects on the oxidation of N-AC. The catalytic peak current obtained by square wave voltammetric was linearly dependent on the N-AC concentrations and the lower quantitation of 0.009μM. The Ni(II)/ZrO_2/NPs/CPE has good selectivity, and is a simple and highly sensitive sensor for the square wave voltammetric determination of N-AC in some real samples such as tablets and urine.

Conflict of interest

All of the authors declare that they have no conflict(s) of interest.

Acknowledgments

The authors thank the Graduate University of Advanced Technology, Kerman, Iran, for their support.

Appendix A. Supplementary data

Supplementary data related to this article can be found at http://dx.doi.org/10.1016/j.jfda.2017.01.003.

REFERENCES

[1] Van Schayck C, Dekhuijzen P, Gorgels W, Van Grunsven P, Molema J, Van Herwaarden C, van Weel C. Are anti-oxidant and anti-inflammatory treatments effective in different subgroups of COPD? A hypothesis. Resp Med 1998;92:1259–64.

[2] Vadoud-Seyedi J, De Dobbeleer G, Simonart T. Treatment of haemodialysis-associated pseudoporphyria with N-acetylcysteine: report of two cases. Br J Dermatol 2000;142:580–1.

[3] Alvarez-Coque MG, Hernandez MM, Camanas RV, Fernandez CM. Spectrophotometric determination of N-acetylcysteine in drug formulations with o-phthalaldehyde and isoleucine. Analyst 1989;114:975–7.

[4] Raggi M, Cavrini V, Di Pietra A. Colorimetric determination of acetylcysteine, penicillamine, and mercaptopropionylglycine in pharmaceutical dosage forms. J Pharm Sci 1982;71:1384–6.

[5] Suarez WT, Vieira HJ, Fatibello-Filho O. Generation and destruction of unstable reagent in flow injection system: determination of acetylcysteine in pharmaceutical formulations using bromine as reagent. J Pharm Biomed Anal 2005;37:771–5.

[6] de Toledo Fornazari AL, Suarez WT, Vieira HJ, Fatibello-Filho O. Flow injection spectrophotometric system for N-acetyl-l-cysteine determination in pharmaceuticals. Acta Chim Slov 2005;52:164–7.

[7] Concha-Herrera V, Torres-Lapasió J, García-Alvarez-Coque M. Chromatographic determination of thiols after pre-column derivatization with o-phthalaldehyde and isoleucine. J Liq Chromatogr R T 2004;27:1593–609.

[8] Tsikas D, Sandmann J, Ikic M, Fauler J, Stichtenoth DO, Frölich JC. Analysis of cysteine and N-acetylcysteine in human plasma by high-performance liquid chromatography at the basal state and after oral administration of N-acetylcysteine. J Chromatogr B 1998;708:55–60.

[9] Tsai F, Chen C, Chien C. Determination of the cysteine derivatives N-acetylcysteine, S-carboxymethylcysteine and methylcysteine in pharmaceuticals by high-performance liquid chromatography. J Chromatogr A 1995;697:309–15.

[10] Suarez WT, Madi AA, Vicentini FC, Fatibello-Filho O. Flow-injection spectrophotometric determination of N-acetylcysteine in pharmaceutical formulations with on-line solid-phase reactor containing Zn(II) phosphate immobilized in a polyester resin. Anal Lett 2007;40:3417–29.

[11] Al-Ghannam SM, El-Brashy A, Al-Farhan B. Fluorimetric determination of some thiol compounds in their dosage forms. Farmaco 2002;57:625–9.

[12] Ensafi AA, Karimi-Maleh H, Mallakpour S, Hatami M. Simultaneous determination of N-acetylcysteine and acetaminophen by voltammetric method using N-(3, 4-dihydroxyphenethyl)-3,5-dinitrobenzamide modified multiwall carbon nanotubes paste electrode. Sens Actuators B Chem 2011;155:464–72.

[13] Arabali V, Karimi-Maleh H, Beitollahi H, Moradi R, Ebrahimi M, Ahmar H. A nanostructure-based electrochemical sensor for square wave voltammetric

determination of N-acetylcysteine in pharmaceutical and biological samples. Ionics 2015;21:1153–61.
[14] Atar N, Eren T, Yola ML, Karimi-Maleh H, Demirdögen B. Magnetic iron oxide and iron oxide@gold nanoparticle anchored nitrogen and sulfur-functionalized reduced graphene oxide electrocatalyst for methanol oxidation. RSC Adv 2015;5:26402–9.
[15] Eren T, Atar N, Yola ML, Karimi-Maleh H. A sensitive molecularly imprinted polymer based quartz crystal microbalance nanosensor for selective determination of lovastatin in red yeast rice. Food Chem 2015;185:430–6.
[16] Karimi-Maleh H, Tahernejad-Javazmi F, Atar N, Yola MLt, Gupta VK, Ensafi AA. A novel DNA biosensor based on a pencil graphite electrode modified with polypyrrole/functionalized multiwalled carbon nanotubes for determination of 6-mercaptopurine anticancer drug. Ind Eng Chem Res 2015;54:3634–9.
[17] Sanghavi BJ, Srivastava AK. Adsorptive stripping differential pulse voltammetric determination of venlafaxine and desvenlafaxine employing Nafion–carbon nanotube composite glassy carbon electrode. Electrochim Acta 2011;56:4188–96.
[18] Sanghavi BJ, Moore JA, Chávez JL, Hagen JA, Kelley-Loughnane N, Chou C-F, Swami NS. Aptamer-functionalized nanoparticles for surface immobilization-free electrochemical detection of cortisol in a microfluidic device. Biosen Bioelectron 2016;78:244–52.
[19] Sanghavi BJ, Mobin SM, Mathur P, Lahiri GK, Srivastava AK. Biomimetic sensor for certain catecholamines employing copper (II) complex and silver nanoparticle modified glassy carbon paste electrode. Biosens Bioelectron 2013;39:124–32.
[20] Sanghavi BJ, Wolfbeis OS, Hirsch T, Swami NS. Nanomaterial-based electrochemical sensing of neurological drugs and neurotransmitters. Microchim Acta 2015;182:1–41.
[21] Atta NF, El-Kady MF, Galal A. Palladium nanoclusters-coated polyfuran as a novel sensor for catecholamine neurotransmitters and paracetamol. Sens Actuators B Chem 2009;141:566–74.
[22] Atta NF, El-Kady MF, Galal A. Simultaneous determination of catecholamines, uric acid and ascorbic acid at physiological levels using poly (N-methylpyrrole)/Pd-nanoclusters sensor. Anal Biochem 2010;400:78–88.
[23] Karimi-Maleh H, Shojaei AF, Tabatabaeian K, Karimi F, Shakeri S, Moradi R. Simultaneous determination of 6-mercaptopruine, 6-thioguanine and dasatinib as three important anticancer drugs using nanostructure voltammetric sensor employing Pt/MWCNTs and 1-butyl-3-methylimidazolium hexafluoro phosphate. Biosens Bioelectron 2016;86:879–84.
[24] Bavandpour R, Karimi-Maleh H, Asif M, Gupta VK, Atar N, Abbasghorbani M. Liquid phase determination of adrenaline uses a voltammetric sensor employing $CuFe_2O_4$ nanoparticles and room temperature ionic liquids. J Mol Liq 2016;213:369–73.
[25] Karimi-Maleh H, Ahanjan K, Taghavi M, Ghaemy M. A novel voltammetric sensor employing zinc oxide nanoparticles and a new ferrocene-derivative modified carbon paste electrode for determination of captopril in drug samples. Anal Methods 2016;8:1780–8.
[26] Sadeghi R, Karimi-Maleh H, Bahari A, Taghavi M. A novel biosensor based on ZnO nanoparticle/1,3-dipropylimidazolium bromide ionic liquid-modified carbon paste electrode for square-wave voltammetric determination of epinephrine. Phys Chem Liq 2013;51:704–14.
[27] Sun W, Yang M, Jiao K. Electrocatalytic oxidation of dopamine at an ionic liquid modified carbon paste electrode and its analytical application. Anal Bioanal Chem 2007;389:1283–91.
[28] Safavi A, Maleki N, Farjami F, Farjami E. Electrocatalytic oxidation of formaldehyde on palladium nanoparticles electrodeposited on carbon ionic liquid composite electrode. J Electroanal Chem 2009;626:75–9.
[29] Sun W, Yang M, Gao R, Jiao K. Electrochemical determination of ascorbic acid in room temperature ionic liquid BPPF6 modified carbon paste electrode. Electroanalysis 2007;19:1597–602.
[30] Beitollah H, Goodarzian M, Khalilzadeh MA, Karimi-Maleh H, Hassanzadeh M, Tajbakhsh M. Electrochemical behaviors and determination of carbidopa on carbon nanotubes ionic liquid paste electrode. J Mol Liq 2012;173:137–43.
[31] Ensafi AA, Izadi M, Karimi-Maleh H. Sensitive voltammetric determination of diclofenac using room-temperature ionic liquid-modified carbon nanotubes paste electrode. Ionics 2013;19:137–44.
[32] Karimi-Maleh H, Rostami S, Gupta VK, Fouladgar M. Evaluation of ZnO nanoparticle ionic liquid composite as a voltammetric sensing of isoprenaline in the presence of aspirin for liquid phase determination. J Mol Liq 2015;201:102–7.
[33] Afsharmanesh E, Karimi-Maleh H, Pahlavan A, Vahedi J. Electrochemical behavior of morphine at ZnO/CNT nanocomposite room temperature ionic liquid modified carbon paste electrode and its determination in real samples. J Mol Liq 2013;181:8–13.
[34] Bijad M, Karimi-Maleh H, Khalilzadeh MA. Application of ZnO/CNTs nanocomposite ionic liquid paste electrode as a sensitive voltammetric sensor for determination of ascorbic acid in food samples. Food Anal Methods 2013;6:1639–47.
[35] Najafi M, Khalilzadeh MA, Karimi-Maleh H. A new strategy for determination of bisphenol A in the presence of Sudan I using a ZnO/CNTs/ionic liquid paste electrode in food samples. Food Chem 2014;158:125–31.
[36] Elyasi M, Khalilzadeh MA, Karimi-Maleh H. High sensitive voltammetric sensor based on Pt/CNTs nanocomposite modified ionic liquid carbon paste electrode for determination of Sudan I in food samples. Food Chem 2013;141:4311–7.
[37] Unnikrishnan B, Yang Y-L, Chen S-M. Amperometric determination of folic acid at multi-walled carbon nanotube-polyvinyl sulfonic acid composite film modified glassy carbon electrode. Int J Electrochem Sci 2011;6:3224–37.
[38] Nakanishi W, Minami K, Shrestha LK, Ji Q, Hill JP, Ariga K. Bioactive nanocarbon assemblies: nanoarchitectonics and applications. Nano Today 2014;9:378–94.
[39] Shayeh JS, Ehsani A, Ganjali M, Norouzi P, Jaleh B. Conductive polymer/reduced graphene oxide/Au nano particles as efficient composite materials in electrochemical supercapacitors. Appl Surf Sci 2015;353:594–9.
[40] Karimi-Maleh H, Biparva P, Hatami M. A novel modified carbon paste electrode based on NiO/CNTs nanocomposite and (9,10-dihydro-9,10-ethanoanthracene-11,12-dicarboximido)-4-ethylbenzene-1,2-diol as a mediator for simultaneous determination of cysteamine, nicotinamide adenine dinucleotide and folic acid. Biosens Bioelectron 2013;48:270–5.
[41] Karimi-Maleh H, Tahernejad-Javazmi F, Ensafi AA, Moradi R, Mallakpour S, Beitollahi H. A high sensitive biosensor based on FePt/CNTs nanocomposite/N-(4-hydroxyphenyl)-3,5-dinitrobenzamide modified carbon paste electrode for simultaneous determination of glutathione and piroxicam. Biosens Bioelectron 2014;60:1–7.

[42] Taşdemir İH. Electrochemistry and determination of cefdinir by voltammetric and computational approaches. J Food Drug Anal 2014;22:527–36.
[43] Nasirizadeh N, Shekari Z, Nazari A, Tabatabaee M. Fabrication of a novel electrochemical sensor for determination of hydrogen peroxide in different fruit juice samples. J Food Drug Anal 2016;24:72–82.
[44] Enríquez JH, Lajas LC, Alamilla RG, Mares AC, Robles GS, Serrano LG. Synthesis and characterization of mesoporous and nano-crystalline phosphate zirconium oxides. J Alloy Compd 2009;483:425–8.
[45] Galus Z. Fundamentals of electrochemical analysis. New York: Ellis Horwood, Halsted Press; 1976.
[46] Fouladgar M, Karimi-Maleh H, Hosseinzadeh R. Novel nanostructured electrochemical sensor for voltammetric determination of N-acetylcysteine in the presence of high concentrations of tryptophan. Ionics 2013;19:665–72.